J|A|C|S
ARTICLES
Published on Web 09/10/2004

Density Functional Theory Studies of the [2]Rotaxane Component of the Stoddart−Heath Molecular Switch

Yun Hee Jang, Sungu Hwang, Yong-Hoon Kim, Seung Soon Jang, and William A. Goddard, III*

Contribution from the Materials and Process Simulation Center, Beckman Institute (139-74), California Institute of Technology, Pasadena, California 91125

Received September 16, 2003; E-mail: wag@wag.caltech.edu

Abstract: The central component of the programmable molecular switch recently demonstrated by Stoddart and Heath is [2]rotaxane, which consists of a cyclobis(paraquat-*p*-phenylene) shuttle $(CBPQT^{4+})(PF_6^-)_4$ (the ring) encircling a finger and moving between two stations, tetrathiafulvalene (TTF) and 1,5-dioxynaphthalene (DNP). As a step toward understanding the mechanism of this switch, we report here its electronic structure using two flavors of density functional theory (DFT): B3LYP/6-31G** and PBE/6-31G**. We find that the electronic structure of composite [2]rotaxane can be constructed reasonably well from its parts by combining the states of separate stations (TTF and DNP) with or without the $(CBPQT)(PF_6)_4$ shuttle around them. That is, the "CBPQT@TTF" state, $(TTF)(CBPQT)(PF_6)_4-(DNP)$, is described well as a combination of the $(TTF)(CBPQT)(PF_6)_4$ complex and free DNP, and the "CBPQT@DNP" state, $(TTF)-(DNP)(CBPQT)(PF_6)_4$, is described well as a combination of free TTF and the $(DNP)(CBPQT)(PF_6)_4$ complex. This allows an aufbau or a "bottom-up" approach to predict the complicated [*n*]rotaxanes in terms of their components. This should be useful in designing new components to lead to improved properties of the switches. A critical function of the $(CBPQT^{4+})(PF_6^-)_4$ shuttle in switching is that it induces a downshift of the frontier orbital energy levels of the station it is on (TTF or DNP). This occurs because of the net positive electrostatic potential exerted by the $CBPQT^{4+}$ ring, which is located closer to the active station than the four PF_6^-'s. This downshift alters the relative position of energy levels between TTF and DNP, which in turn alters the electron tunneling rate between them, even when the shuttle is *not* involved directly in the actual tunneling process. Based on this switching mechanism, the "CBPQT@TTF" state is expected to be a better conductor since it has better aligned levels between the two stations. A second potential role of the $(CBPQT^{4+})(PF_6^-)_4$ shuttle in switching is to provide low-lying LUMO levels. If the shuttle is involved in the actual tunneling process, the reduced HOMO−LUMO gap (from 3.6 eV for the isolated finger to 1.1 eV for "CBPQT@TTF" or to 0.6 eV for "CBPQT@DNP" using B3LYP) would significantly facilitate the electron tunneling through the system. This might occur in a folded conformation where a direct contact between free station and the shuttle on the other station is possible. When this becomes the main switching mechanism, we expect the "CBPQT@DNP" state to become a better conductor because its HOMO−LUMO gap is smaller and because its HOMO and LUMO are localized at different stations (HOMO exclusively at TTF and LUMO at CBPQT encircling DNP) so that the HOMO-to-LUMO tunneling would be through the entire molecule of [2]rotaxane. Thus an essential element in designing these switches is to determine the configuration of the molecules (e.g., through self-assembled monolayers or incorporation of conformation stabilizing units).

1. Introduction

One of the most exciting developments in science and technology over the past few years is molecular electronics, in which new molecular components [switches, rectifiers, transistors, interconnects (wires), memories, etc.] are designed for nanomanufacturing (chemical assembly) of electronic devices (solid-state electronic devices composed of self-assembled monolayers or single-molecule junctions).[1−7]

One of the most promising candidates for a programmable molecular switch is a self-assembled monolayer (SAM) of the "Stoddart−Heath type" bistable [2]rotaxane (**1**) anchored on a metal [e.g., onto gold with disulfide bonds or onto polysilicon electrodes with poly(ethylene oxide)-type anchors][2,5] (alternatively one might consider the [2]catenane relative).[8,9] It is thought that this type of switch is turned on and off reversibly

(1) Carroll, R. L.; Gorman, C. B. *Angew. Chem., Int. Ed.* **2002**, *41*, 4378−4400.
(2) Heath, J. R.; Ratner, M. A. *Phys. Today* **2003**, *56*, 43−49.
(3) Reed, M. A.; Tour, J. M. *Sci. Am.* **2000**, *282*, 86−93.
(4) Joachim, C.; Gimzewski, J. K.; Aviram, A. *Nature* **2000**, *408*, 541−548.
(5) Luo, Y.; Collier, C. P.; Jeppensen, J. O.; Nielsen, K. A.; Delonno, E.; Ho, G.; Perkins, J.; Tseng, H.-R.; Yamamoto, T.; Stoddart, J. F.; Heath, J. R. *ChemPhysChem* **2002**, *3*, 519−525.
(6) Collier, C. P.; Wong, E. W.; Belohradsky, M.; Raymo, F. M.; Stoddart, J. F.; Kuekes, P. J.; Williams, R. S.; Heath, J. R. *Science* **1999**, *285*, 391−394.
(7) Wong, E. W.; Collier, C. P.; Behloradsky, M.; Raymo, F. M.; Stoddart, J. F.; Heath, J. R. *J. Am. Chem. Soc.* **2000**, *122*, 5831−5840.

10.1021/ja0385437 CCC: $27.50

upon moving the cyclobis(paraquat-*p*-phenylene) ($CBPQT^{4+}$; blue ring) shuttle between the tetrathiafulvalene (TTF; green station) and the 1,5-dioxynaphthalene (DNP; red station) by oxidation and reduction of the TTF.[10,11] However, the fundamental understanding of the switching mechanism of **1** needed to derive design principles to improve switching components is lacking,[1] especially for the solid-state devices.[5]

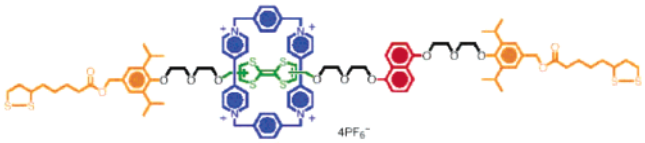

1

There have been previous theoretical studies on the Stoddart−Heath type rotaxanes, using both quantum-mechanics (QM)[12−14] and force-field (FF)[15−18] approaches, but the emphasis has been on the complexation of the CBPQT ring with simple aromatic compounds (benzenes and biphenyls)[12−16,18] with one study on the energy barrier for shuttling between two such stations connected via polyether units[17] and another on the conformation of a different but related type of rotaxane.[18] However, there has been little effort to establish the origin of the "on−off" switching behavior accompanied by changing the ring position.[19]

Here we build up a knowledge of the switching mechanism from theory using an aufbau or "bottom-up" analysis. We first calculate the electronic structures using quantum mechanics (QM) for the simplest models representing the basic components of **1** to establish the role of each component in conduction (or switching), and then we combine and extend these results to more realistic models of the systems studied experimentally. Thus we consider here (Figure S1, Supporting Information):

(a) Each station, TTF and DNP (Figure 1, section 3.1);

(b) The complex of the shuttle with each station, (TTF)-$(CBPQT)(PF_6)_4$ and (DNP)$(CBPQT)(PF_6)_4$ (Figure 3, section 3.2);

(c) The isolated finger connecting two stations, TTF-DNP (Figure 7, section 3.3);

(d) Complexes in which the shuttle sits at one of the stations in the finger, (TTF)$(CBPQT)(PF_6)_4$−(DNP) and (TTF)−(DNP)-$(CBPQT)(PF_6)_4$ (Figure 10, section 3.4).

We find a simple description on how the threading process affects the electronic structure of a series of stations, which provides the basis for understanding the electron tunneling

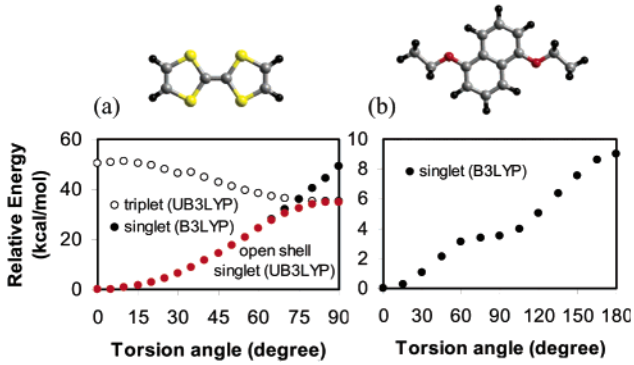

Figure 1. Potential energy (restricted or unrestricted B3LYP/6-31G**) for (a) the torsion around the central C═C bond of TTF and (b) the rotation of the ethoxy group away from the naphthalene plane of ethoxynaphthalene (and DNP). Each case has one minimum, the planar configuration shown. Color code: yellow (S), red (O), gray (C), and black (H).

(conductance) through them. A specific question here is what role the $CBPQT^{4+}$ shuttle plays. Does the current flow through it? This would require strong matrix elements coupling the $CBPQT^{4+}$ ring and the station(s). Or does the current flow only through the thread of each station, without directly involving the ring in tunneling? This might occur if the overlap between the ring and the stations is negligible. In this case, we show below that the $CBPQT^{4+}$ ring can still control the electron flow by providing a strong positive electrostatic field inside the station to modulate the relative energy levels of the stations.

The results reported here provide the basis for extensions: Additional components such as the poly(ethylene oxide) linker between two stations can be added to the current simple model to allow the greater conformational flexibility of the experimental systems, and the model compounds optimized in this study can be attached to conducting electrodes (e.g., gold) by including anchors (e.g., thiols) at both ends to calculate the current−voltage ($I-V$) curve.[20−22] Since the $I-V$ characteristics depend significantly on the structure (intermolecular packing as well as intramolecular conformation) of molecules on the electrodes,[20] either QM or a FF based on the QM data can be used in molecular dynamics (MD) simulations to determine the optimum coverage and configuration of the SAM of the model compounds on a metal surface.

2. Calculation Details

The initial structure of each model system [TTF, DNP, CBPQT, (TTF)(CBPQT), (DNP)(CBPQT)] was taken from X-ray crystallographic structures.[23−26] A full geometry optimization in QM was carried out using the B3LYP[27−31] flavor of DFT with the 6-31G** basis

(8) Collier, C. P.; Mattersteig, G.; Wong, E. W.; Luo, Y.; Beverly, K.; Sampaio, J.; Raymo, F. M.; Stoddart, J. F.; Heath, J. R. *Science* **2000**, *289*, 1172−1175.
(9) Pease, A. R.; Jeppesen, J. O.; Stoddart, J. F.; Luo, Y.; Collier, C. P.; Heath, J. R. *Acc. Chem. Res.* **2001**, *34*, 433−444.
(10) Balzani, V.; Credi, A.; Mattersteig, G.; Matthews, O. W.; Raymo, F. M.; Stoddart, J. F.; Venturi, M.; White, A. J. P.; Williams, D. J. *J. Org. Chem.* **2000**, *65*, 1924−1936.
(11) Tseng, H.-R.; Vignon, S. A.; Stoddart, J. F. *Angew. Chem., Int. Ed.* **2003**, *42*, 1491−1495.
(12) Zhang, K.-C.; Liu, L.; Mu, T.-W.; Guo, Q.-X. *Chem. Phys. Lett.* **2001**, *333*, 195−198.
(13) Macias, A. T.; Kumar, K. A.; Marchand, A. P.; Evanseck, J. D. *J. Org. Chem.* **2000**, *65*, 2083−2089.
(14) Castro, R.; Berardi, M. J.; Cordova, E.; de Olza, M. O.; Kaifer, A. E.; Evanseck, J. D. *J. Am. Chem. Soc.* **1996**, *118*, 10257−10268.
(15) Grabuleda, X.; Ivanov, P.; Jaime, C. *J. Org. Chem.* **2003**, *68*, 1539−1547.
(16) Kaminski, G. A.; Jorgensen, W. L. *J. Chem. Soc., Perkin Trans. 2* **1999**, 2365−2375.
(17) Grabuleda, X.; Jaime, C. *J. Org. Chem.* **1998**, *63*, 9635−9643.
(18) Zheng, X.; Sohlberg, K. *J. Phys. Chem. A* **2003**, *107*, 1207−1215.
(19) Deng, W.-Q.; Muller, R. P.; Goddard, W. A., III. *J. Am. Chem. Soc.*, in press.
(20) Nitzan, A.; Ratner, M. A. *Science* **2003**, *300*, 1384−1389.
(21) Brandbyge, M.; Mozos, J.-L.; Ordejon, P.; Taylor, J.; Stokbro, K. *Phys. Rev. B* **2002**, *65*, 165401.
(22) Xue, Y.; Datta, S.; Ratner, M. A. *J. Chem. Phys.* **2001**, *115*, 4292−4299.
(23) Philp, D.; Slawin, A. M. Z.; Spencer, N.; Stoddart, J. F.; Williams, D. J. *J. Chem. Soc., Chem. Commun.* **1991**, 1584−1586.
(24) Reddington, M. V.; Slawin, A. M. Z.; Spencer, N.; Stoddart, J. F.; Vincent, C.; Williams, D. J. *J. Chem. Soc., Chem. Commun.* **1991**, 630−634.
(25) Odell, B.; Reddington, M. V.; Slawin, A. M. Z.; Spencer, N.; Stoddart, J. F.; Williams, D. J. *Angew. Chem., Int. Ed. Engl.* **1988**, *27*, 1547−1550.
(26) Anelli, P. L.; Ashton, P. R.; Ballardini, R.; Balzani, V.; Delgado, M.; Gandolfi, M. T.; Goodnow, T. T.; Kaifer, A. E.; Philp, D.; Pietraszkiewicz, M.; Prodi, L.; Reddington, M. V.; Slawin, A. M. Z.; Spencer, N.; Stoddart, J. F.; Vicent, C.; Williams, D. J. *J. Am. Chem. Soc.* **1992**, *114*, 193−218.
(27) Slater, J. C. *Quantum Theory of Molecules and Solids. Vol. 4. The Self-Consistent Field for Molecules and Solids*; McGraw-Hill: New York, 1974.
(28) Becke, A. D. *Phys. Rev. A* **1988**, *38*, 3098−3100.
(29) Vosko, S. H.; Wilk, L.; Nusair, M. *Can. J. Phys.* **1980**, *58*, 1200−1211.
(30) Lee, C.; Yang, W.; Parr, R. G. *Phys. Rev. B* **1988**, *37*, 785−789.

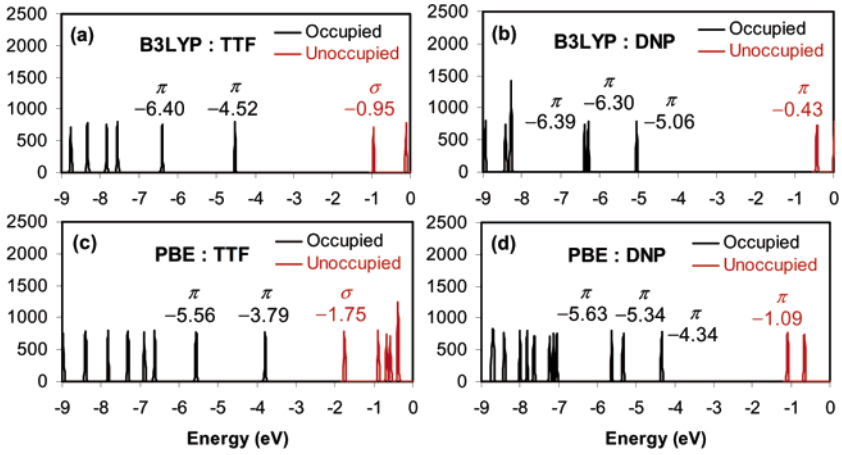

Figure 2. Density of states from DFT calculations. (a) TTF using B3LYP/6-31G**, (b) DNP using B3LYP/6-31G**, (c) TTF using PBE/6-31G**, and (d) DNP using PBE/6-31G**. TTF has a higher HOMO and a lower LUMO (that is, smaller HOMO−LUMO gap) than DNP for both flavors of DFT. PBE gives a smaller HOMO−LUMO gap than B3LYP for both compounds.

set. At the final geometry the electronic structure was analyzed by the density of states (DOS), the density of states projected to each component (PDOS),[32] and the visualized molecular orbitals (MOs). *Since the unoccupied MOs* (represented in red in following figures) *are not very reliably described in DFT, we use them here only for qualitative analysis.*

To establish which features are sensitive to the calculations, we also carried out single-point energy calculations with another flavor of DFT, PBE[33,34]/6-31G**. This makes sure that our conclusions are independent of functional. These results are summarized in section 3.6 and as Supporting Information.

All calculations were done in the gas phase, using Jaguar v4.2 (B3LYP) and v5.0 (PBE).[35]

3. Results and Discussion

3.1. TTF and DNP. The flexible parts of TTF and DNP are the S−C═C−S bond of TTF and the C═C−O−C bond of DNP. The planar conformation (at 0°) is the only minimum conformation for both TTF and DNP (Figure 1), and hence we analyzed in detail only these conformations. [In addition, TTF has a second "boat-shaped" minimum conformation[36,37] that we calculate to be within 0.01 kcal/mol, the nonplanarity is quite small (12° out-of-plane), and the geometric/electronic structures of the two conformations are very similar (Figure S19).]

The energy levels of the frontier molecular orbitals (FMOs; several HOMOs and LUMOs) of free TTF and free DNP are shown in Figure 2, where the density of states (DOS) represents the number of energy levels (MOs) of a compound between E and $E + dE$,[32]

$$\mathrm{DOS}(E)\,dE = \sum_k \delta(E - E_k)$$

E_k denotes the eigenvalue of the k-th MO. Each peak corresponds to an MO (which was visualized in Figures S2 and S3 of Supporting Information), with black peaks indicating occupied MOs and red peaks indicating unoccupied MOs. [The DOS curves were obtained by broadening the discrete eigenvalues into bands with a Gaussian convolution with 0.0136 eV as the broadening parameter σ and the energy step dE.]

For TTF, the two highest occupied MOs (HOMO and HOMO−1) are both of π character (Figures 2a and S2) and located at −4.52 and −6.40 eV. The lowest unoccupied MO (LUMO) has σ character and is at −0.95 eV. These MOs are delocalized over the whole molecule. Other FMOs such as HOMO−2 (−7.55 eV), HOMO−3 (−7.88 eV), and LUMO+1 (−0.11 eV) are π-type combinations of the sulfur lone pairs. The relative energies between those occupied levels (0.00, 1.88, 3.03, and 3.36 eV with respect to HOMO) are correlated well with those observed in a photoelectron spectroscopy (0.00, 1.88, 3.01, and 3.39 eV).[38]

For DNP, three highest occupied MOs (HOMO, HOMO−1, and HOMO−2), all π orbitals (Figure 2b and Figure S3), are located at −5.06, −6.30, and −6.39 eV. The LUMO at −0.43 eV has π character.

Figure 2c and d show the results using the PBE density functional, which gives higher HOMOs (−3.79, −5.56, −6.62, and −6.89 eV for TTF) and lower LUMOs (−1.75 and −0.89 eV for TTF). This leads to a smaller HOMO−LUMO gap than B3LYP but has essentially the same MO characters. A detailed analysis of electronic structure based on the PBE functional is summarized in section 3.6 and in section B of the Supporting Information.

We note that both flavors of DFT give a higher HOMO and a lower LUMO (that is, smaller HOMO−LUMO gap) for TTF than for DNP. This is consistent with experimental measurements of ionization potential (6.7 eV for TTF[38,39] and 7.4 eV for 1,5-dimethoxynaphthalene[40]) and redox potential (0.3−0.4 V vs SCE for TTF in acetonitrile[10,38,41] and 1.1−1.3 V for 1,5-dimethoxynaphthalene[10,41,42]). Thus, if connecting TTF and DNP

(31) Miehlich, B.; Savin, A.; Stoll, H.; Preuss, H. *Chem. Phys. Lett.* **1989**, *157*, 200−206.
(32) Hoffmann, R. *Solids and Surfaces: a Chemist's View of Bonding in Extended Structures*; VCH: New York, 1988.
(33) Perdew, J. P.; Burke, K.; Ernzerhof, M. *Phys. Rev. Lett.* **1996**, *77*, 3865−3868.
(34) Perdew, J. P.; Burke, K.; Ernzerhof, M. *Phys. Rev. Lett.* **1997**, *78*, 1396−1396.
(35) Schrodinger Inc.: Portland, OR, 2003.
(36) Hargittai, I.; Brunvoll, J.; Kolonits, M.; Khodorkovsky, V. *J. Mol. Struct.* **1994**, *317*, 273−277.
(37) Pou-Amerigo, R.; Orti, E.; Merchan, M.; Rubio, M.; Viruela, P. M. *J. Phys. Chem. A* **2002**, *106*, 631−640.
(38) Lichtenberger, D. L.; Johnston, R. L.; Hinkelmann, K.; Suzuki, T.; Wudl, F. *J. Am. Chem. Soc.* **1990**, *112*, 3302−3307.
(39) Saito, G.; Enoki, T.; Mototada, K.; Imaeda, K.; Sato, N.; Inokuchi, H. *Mol. Cryst. Liq. Cryst.* **1985**, *119*, 393−400.
(40) El-Kemary, M. A. *Can. J. Appl. Spectrosc.* **1996**, *41*, 109−113.
(41) Ashton, P. R.; Baldoni, V.; Balzani, V.; Claessens, C. G.; Credi, A.; Hoffmann, H. D. A.; Raymo, F. M.; Stoddart, J. F.; Venturi, M.; White, A. J. P.; Williams, D. J. *Eur. J. Org. Chem.* **2000**, 1121−1130.
(42) Zweig, A.; Maurer, A. H.; Roberts, B. G. *J. Org. Chem.* **1967**, *32*, 1322−1329.

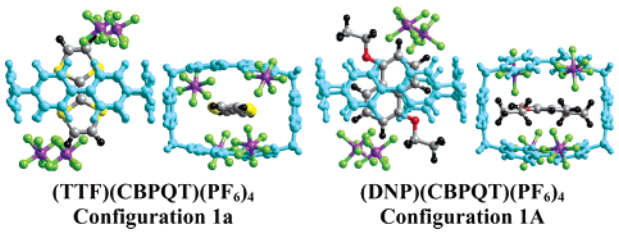

Figure 3. Side and top view of the optimized structures for (TTF)(CBPQT)-$(PF_6)_4$ and (DNP)(CBPQT)$(PF_6)_4$. Color code: yellow (S), gray (C), black (H), purple (P), light green (F), and light blue (CBPQT).

to each other does not perturb the electronic structure of those units, we would expect that the HOMO and LUMO of the entire system would correspond to TTF, and the next FMO's (HOMO−1 and LUMO+1) would correspond to DNP. Indeed below (section 3.3) we find this to be the case.

3.2. Complex between (CBPQT)$(PF_6)_4$ and TTF/DNP. The next question concerns the role of the shuttle ring, (CBPQT)-$(PF_6)_4$, in the rotaxane molecular switch. We investigated the change in the electronic structure of each station (TTF and DNP) caused by its complexation with (CBPQT)$(PF_6)_4$.

We started with the X-ray crystallographic structures of (TTF)(CBPQT)$(PF_6)_4$ and (DNP)(CBPQT)$(PF_6)_4$.[23,24] Then we fully optimized the geometry using QM (B3LYP/6-31G**) (Figures S4 and S5 of Supporting Information). The most favorable configuration of the PF_6^- units has a pair of PF_6^-'s above the hole of the CBPQT ring and another pair below it (**Configuration 1**'s and **2**'s). Among two possible orientations of DNP relative to the CBPQT ring of (DNP)(CBPQT)$(PF_6)_4$, **Configuration 1A** (with the naphthalene of DNP out of phase with the paraquat of CBPQT, as found in the crystal structures[24,43,44]) is more stable than **Configuration 1B** (where they are parallel to each other). Among several minimum-energy configurations thus identified [**Configuration 1a**, **1b**, and **2** for (TTF)(CBPQT)$(PF_6)_4$; **Configuration 1A** and **2A** for (DNP)-(CBPQT)$(PF_6)_4$], which have comparable energies and *qualitatively* similar electronic structures (compare Figure S18a with S18a′ and Figure S18b with S18b′ in Supporting Information), we here show the detailed analysis only for **Configuration 1a** of (TTF)(CBPQT)$(PF_6)_4$ and **Configuration 1A** of (DNP)-(CBPQT)$(PF_6)_4$ (Figure 3), because the arrangements of their components (especially, four PF_6's) are quite similar to each other. This allows us to carry out the comparative analysis of their electronic structures safely without geometric factors.

Figure 4a shows the DOS of the (TTF)(CBPQT)$(PF_6)_4$ complex (**Configuration 1a**) along with its projection onto each

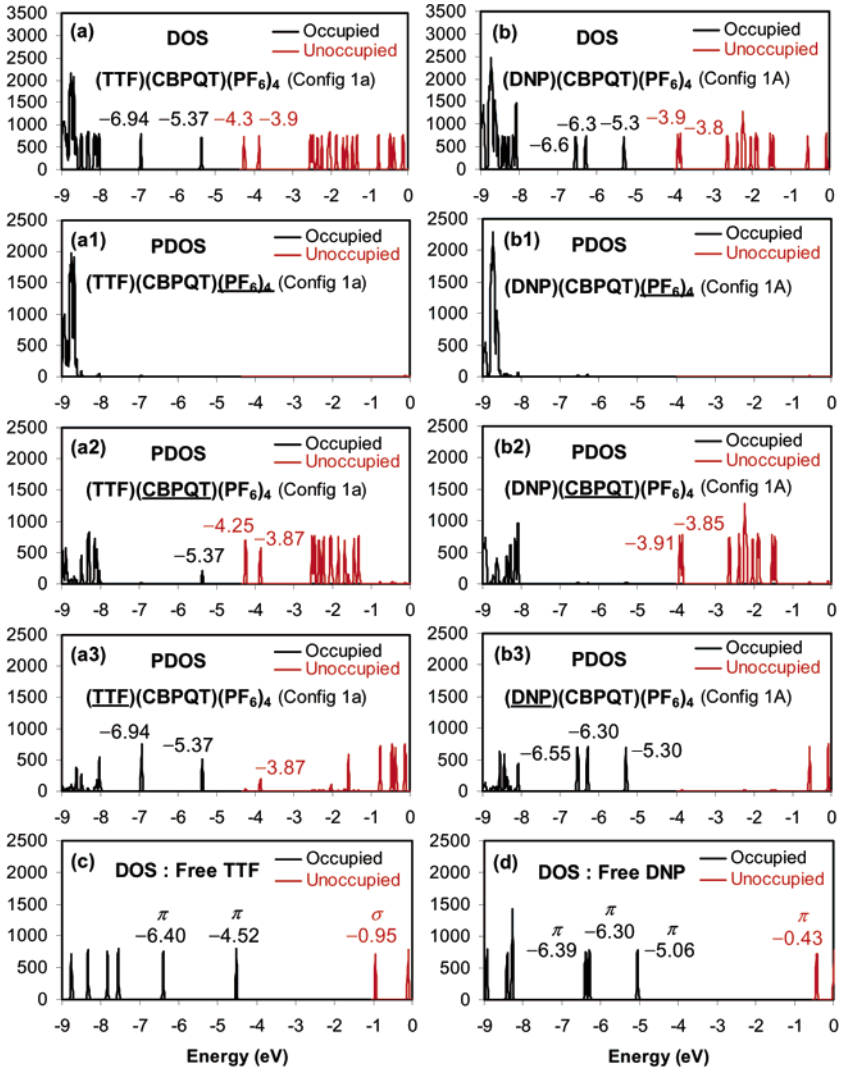

Figure 4. (a) DOS of (TTF)(CBPQT)$(PF_6)_4$ in **Configuration 1a** and (b) DOS of (DNP)(CBPQT)$(PF_6)_4$ in **Configuration 1A**. These figures include the PDOS of each fragment (TTF/DNP, CBPQT, and PF_6) shown together. (c) DOS of free TTF. (d) DOS of free DNP.

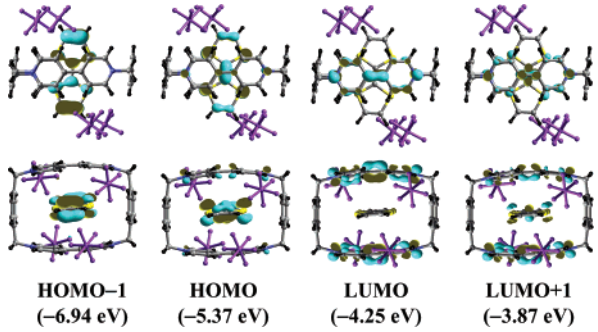

Figure 5. FMOs of (TTF)(CBPQT)$(PF_6)_4$. Color code: yellow (S), blue (N), gray (C), black (H), and purple (PF_6^-).

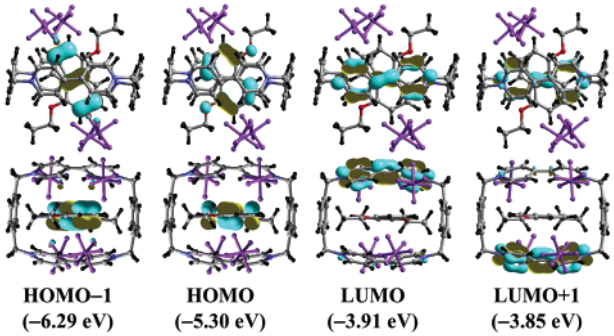

Figure 6. FMOs of (DNP)(CBPQT)$(PF_6)_4$. Color code: red (O), blue (N), gray (C), black (H), and purple (PF_6^-).

fragment (TTF, CBPQT, and PF_6) (projected DOS; PDOS),[32]

$$\mathrm{PDOS(fragment\ A)}(E)\,\mathrm{d}E = \sum_{i\in \mathrm{A}}\sum_{k}\sum_{j} C_{ik}C_{jk}S_{ij}\delta(E - E_k)$$

where C_{ik} denotes the i-th coefficient of the k-th MO and S_{ij} denotes the overlap between the i-th AO (atomic orbital) and the j-th AO. Each peak represents the contribution of each fragment to the total DOS between E and $E + \mathrm{d}E$, which can be confirmed by the visualized MOs shown in Figures 5 and 6 (also in Figures S6 and S7 of the Supporting Information). The DOS of free TTF shown in Figure 4c can be compared with the PDOS of TTF in the complex (Figure 4a3) to reveal how the (CBPQT)$(PF_6)_4$ affects the electronic structure of TTF. The main features are as follows:

(1) The HOMO of the complex (−5.37 eV) corresponds to TTF slightly mixed with CBPQT;

(2) HOMO−1 (−6.94 eV) corresponds purely to TTF;

(3) These energy levels are lowered significantly from those of free TTF (−4.52 and −6.40 eV) by 0.85 and 0.54 eV, respectively;

(4) The LUMO (−4.25 eV) corresponds exclusively to CBPQT;

(5) LUMO+1 (−3.87 eV) corresponds to CBPQT slightly mixed with TTF;

(6) Due to those new low-level LUMO's from CBPQT, the HOMO−LUMO gap of the complex (1.12 eV) is much smaller than that of free TTF (3.57 eV);

(7) CBPQT and PF_6 do not have a significant contribution to the occupied frontier MO's of the complex (until down to −8 eV).

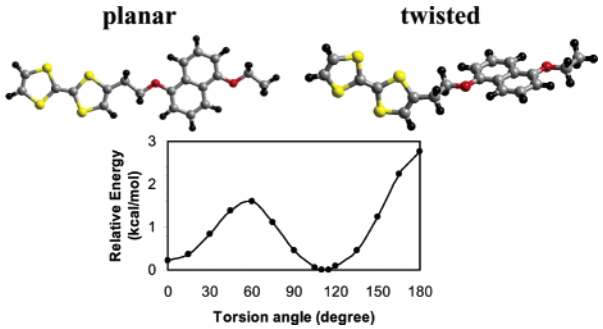

Figure 7. Torsion potential energy curve about the C_2 alkane bridge [the dihedral C═C(from TTF)−C−C(from DNP)] of the TTF−DNP simple connection from DFT (B3LYP/6-31G**). The two minimum conformations, planar (0°) and twisted (115°), are shown above the energy curve. The planar case is 0.2 kcal/mol above the twisted one. Color code: yellow (S), red (O), gray (C), and black (H).

The DOS of the (DNP)(CBPQT)$(PF_6)_4$ complex (**Configuration 1A**) shown in Figure 4b shares the main features (1)−(7) above. However, (CBPQT)$(PF_6)_4$ interacts less strongly with DNP than with TTF: there is essentially no overlap in the PDOS between DNP and (CBPQT)$(PF_6)_4$, indicating essentially no mixing between these two components as also seen in Figure 6. The downshift of energy levels due to (CBPQT)$(PF_6)_4$ is less significant for DNP (0.25 eV) than for TTF (0.85 eV). [The magnitude of the downshift is similar (∼0.6 eV) both for (TTF)-(CBPQT)$(PF_6)_4$ and (DNP)(CBPQT)$(PF_6)_4$ in the alternative most favorable configurations, **Configuration 1b** and **Configuration 2A**, respectively, as shown in the Supporting Information (Figures S18a′ and S18b′). However, other main features did not change.] Thus, the main features for (DNP)(CBPQT)-$(PF_6)_4$ are as follows:

(1) HOMO, HOMO−1, and HOMO−2 (−5.30, −6.29, and −6.55 eV) exclusively correspond to DNP;

(2) These HOMO levels are only slightly lower than those of free DNP (−5.06, −6.30, and −6.39 eV);

(3) Almost degenerate LUMO and LUMO+1 (−3.91 and −3.85 eV) correspond to CBPQT with a negligible mixing with DNP, thus not showing any splitting as shown in the TTF case;

(4) Due to those new low-level LUMOs from CBPQT, the HOMO−LUMO gap of the complex (1.39 eV) is much smaller than that of free DNP (4.62 eV);

(5) Again, CBPQT and PF_6 do not have a significant contribution to the occupied frontier MOs of the complex (until down to −8 eV).

3.3. TTF−DNP Finger without the Ring: Model [2]-Rotaxane − Stations Only. To form a simple model for coupling the stations in [2]rotaxane, we connected TTF and DNP to each other through a C_2 alkane (CH_2−CH_2) bridge as in Figure 7. We find that the new C═C(from TTF)−C−C(from DNP) torsion has two minima at 0° (planar) and at 115° (twisted) with almost the same energy (115° is favored only by 0.2 kcal/mol) (Figure 7), the electronic structure of this TTF−DNP was analyzed for both conformations (Figure 8). We found essentially the same characteristics for both conformations.

The DOS and its projection (PDOS) onto each component is shown in Figure 8. Despite the direct connection between TTF and DNP and the ideal planar conformation, Figure 8a reveals

(43) Asakawa, M.; Dehaen, W.; L'abbe, G.; Menzer, S.; Nouwen, J.; Raymo, F. M.; Stoddart, J. F.; Williams, D. J. *J. Org. Chem.* **1996**, *61*, 9591−9595.

(44) Ashton, P. R.; Brown, C. L.; Chrystal, E. J. T.; Goodnow, T. T.; Kaifer, A. E.; Parry, K. P.; Philp, D.; Slawin, A. M. Z.; Spencer, N.; Stoddart, J. F.; Williams, D. J. *J. Chem. Soc., Chem. Commun.* **1991**, 634−639.

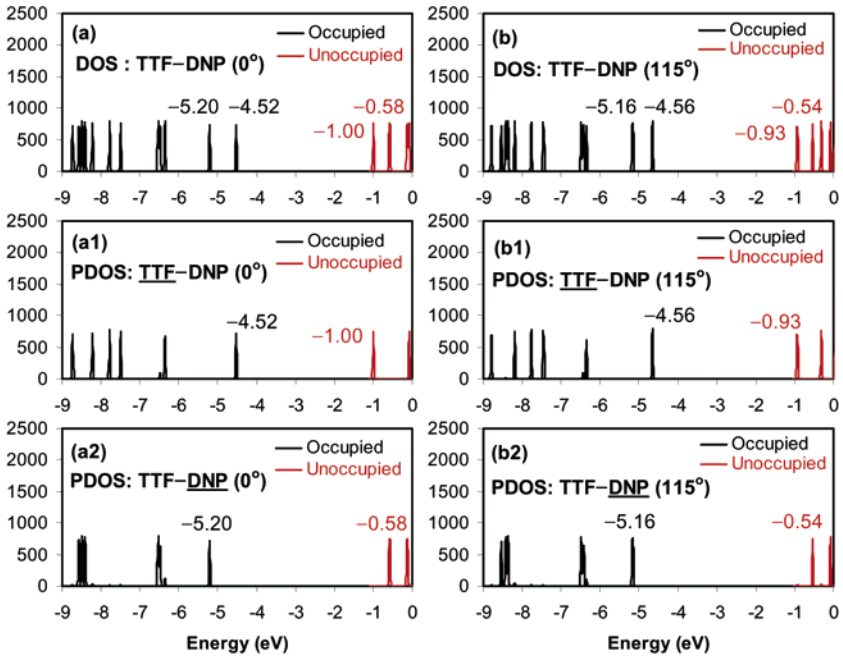

Figure 8. DOS and PDOSs (B3LYP/6-31G**) of TTF−DNP in two conformations: (a) planar and (b) twisted.

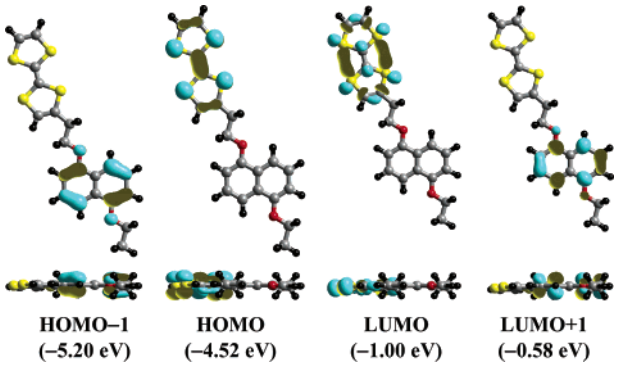

Figure 9. FMOs of TTF−DNP (B3LYP/6-31G**). Color code: yellow (S), red (O), gray (C), and white (H).

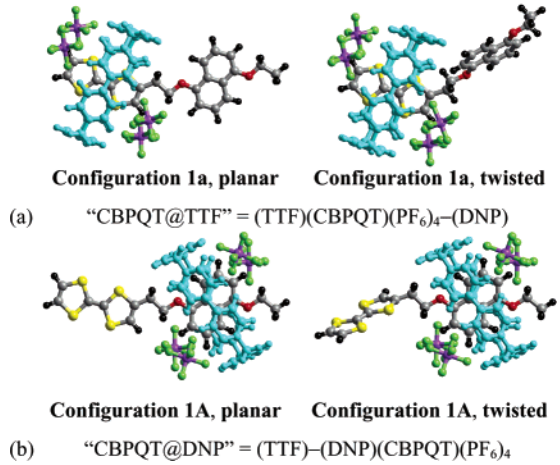

Figure 10. Optimized structure of (a) (TTF)(CBPQT)$(PF_6)_4$−(DNP) in **Configuration 1a** and (b) (TTF)−(DNP)(CBPQT)$(PF_6)_4$ in **Configuration 1A**. The two stations (TTF and DNP) were connected to each other through the C_2 alkane in a planar (left) or twisted (right) conformation. Color code: yellow (S), red (O), gray (C), black (H), purple (P), light green (F), and light blue (CBPQT).

essentially no overlap of wave function between these two units (no overlap in the PDOSs) for the four FMOs (HOMO−1, HOMO, LUMO, and LUMO+1). Thus the identity of each individual unit is preserved, as also shown in the FMOs lined in Figure 9.

(1) The HOMO [−4.52 (planar); −4.56 eV (twisted)] is from the HOMO (−4.52 eV) of free TTF.

(2) The LUMO [−1.00 (planar); −0.93 eV (twisted)] is from the LUMO (−0.95 eV) of free TTF.

(3) HOMO−1 [−5.20 (planar); −5.16 eV (twisted)] is from the HOMO (−5.05 eV) of free DNP.

(4) LUMO+1 [−0.58 (planar); −0.54 eV (twisted)] is from LUMO (−0.43 eV) of free DNP.

Thus the DOS of TTF−DNP is essentially a simple sum of those of free TTF and free DNP, shown in Figure 2, except that the energy levels of DNP are slightly downshifted.

On the other hand, the deeper FMOs, HOMO−2 to HOMO−4, at around −6.5 eV do show some minor mixing between two units.

This overall "conservation-of-identity" and "sum-of-pieces" picture should be even more valid for rotaxanes where the stations are more separated from each other by such linkers as two monomer units of ethylene oxide (−OCH_2CH_2−), *if they are unfolded*. This model allows us to consider the electronic structure of rotaxanes as the direct sum of those of each station with or without the shuttle on it. For example, the Stoddart type [2]rotaxane with the CBPQT shuttle at the TTF station, (TTF)-(CBPQT)$(PF_6)_4$−(DNP), can be described as the sum of the DOS of (TTF)(CBPQT)$(PF_6)_4$ and that of free DNP, and the same type of [2]rotaxane with CBPQT at DNP, (TTF)−(DNP)-(CBPQT)$(PF_6)_4$, can be described as the sum of the DOS of free TTF and that of (CBPQT)(DNP)$(PF_6)_4$, all of which are given altogether in Figure 4. In the following section we will determine how valid this simple view is for these more complicated systems. If valid, this "sum rule" enables us to analyze the electronic structure of intractably complicated

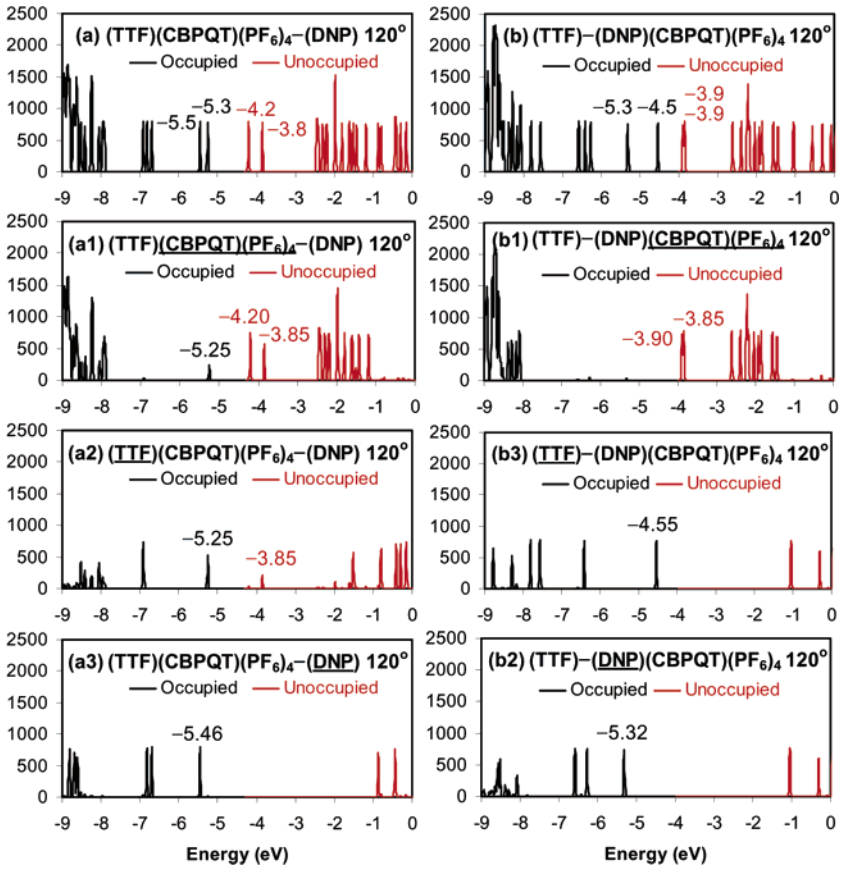

Figure 11. DOSs and PDOSs (B3LYP/6-31G**) of the twisted conformation of (a) (TTF)(CBPQT)$(PF_6)_4$−(DNP) and (b) (TTF)−(DNP)(CBPQT)$(PF_6)_4$.

compounds such as [*n*]rotaxanes in a "bottom-up" fashion, that is, as the combination of the electronic structures of simple pieces.

3.4. Complex between (CBPQT)$(PF_6)_4$ and TTF-DNP Finger: Model [2]Rotaxane. 3.4.1. Validity of the "Sum Rule" for Two Conformations. The (CBPQT)$(PF_6)_4$ shuttle was positioned around either TTF or DNP of TTF−DNP and the geometry was fully optimized using DFT (B3LYP/6-31G**), leading to the final structures shown in Figure 10. We analyzed the difference in the electronic structure between (TTF)-(CBPQT)$(PF_6)_4$−(DNP) and (TTF)−(DNP)(CBPQT)$(PF_6)_4$.

The initial geometric structures were constructed from the optimized structures of (TTF)(CBPQT)$(PF_6)_4$ and (DNP)-(CBPQT)$(PF_6)_4$ using the favorable arrangement of PF_6^-'s around $CBPQT^{4+}$ (**Configuration 1a** and **Configuration 1A**, respectively) and the optimized structures of TTF−DNP finger in both the planar (0°) and the twisted (now optimized to be 120°) conformations.

After optimization, (TTF)(CBPQT)$(PF_6)_4$−(DNP) favors the twisted conformation by 3.1 kcal/mol, while (TTF)−(DNP)-(CBPQT)$(PF_6)_4$ favors the **planar** conformation by 1.1 kcal/mol.

Figure S8 of Supporting Information shows the DOS of (TTF)−(DNP)(CBPQT)$(PF_6)_4$ in both conformations. We see essentially the same characteristics, because the uncomplexed TTF unit stays away both from CBPQT and from the PF_6's in both conformations, retaining its own identity. Indeed, the DOS is essentially the sum of the DOS of free TTF and that of (DNP)-(CBPQT)$(PF_6)_4$ (Figure S8c of Supporting Information), *confirming the "**sum rule**" that the connection does not perturb the electronic structure* of the TTF station and the DNP station even in the presence of the shuttle around one of them, preserving their individual identities.

For (TTF)(CBPQT)$(PF_6)_4$−(DNP) the DOS of both conformations (Figure S9 of Supporting Information) look almost the same, *except that* for the twisted conformation the MOs corresponding to DNP are downshifted slightly (∼ 0.4 eV) but uniformly. This is probably because the uncomplexed DNP in the twisted conformation is close enough to the $CBPQT^{4+}$ ring (Figure 10a) to provide electrostatic potentials that stabilize the energy levels of the DNP, whereas in the planar conformation it is too far from the ring. Indeed, whereas the DOS of the planar conformation is represented well by the sum of those of individual parts, (TTF)(CBPQT)$(PF_6)_4$ and free DNP (Figures S9a and S9c), this is not the case for the twisted conformation (Figures S9b and S9c). Here the main difference lies mostly in the uniform downshift in the energy levels of uncomplexed DNP, which in the complex is positioned next to the $CBPQT^{4+}$ ring.

In the [2]rotaxane on which experiments have been reported, TTF and DNP are connected to each other via an ethylene oxide linker [$(CH_2CH_2O)_3$], which likely prefers a twisted conformation of the thread between stations, with the partially negative ethylene oxide linker crawling around the partially positive corner of the $CBPQT^{4+}$ ring. Thus the uncomplexed DNP in the "CBPQT@TTF" state of the synthesized [2]rotaxane very likely sits close by the $CBPQT^{4+}$ ring.[45] Consequently we

(45) Yamamoto, T.; Tseng, H.-R.; Stoddart, J. F.; Balzani, V.; Credi, A.; Marchioni, F.; Venturi, M. *Collect. Czech. Chem. Commun.* **2003**, *68*, 1488−1514.

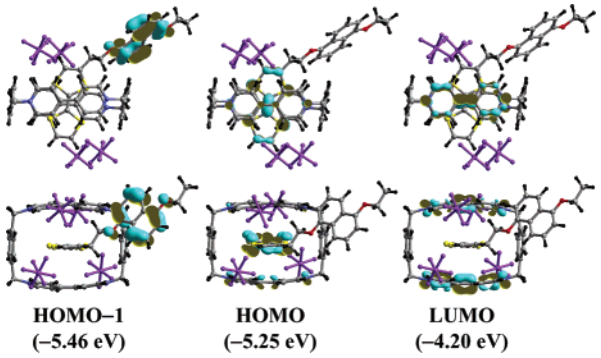

Figure 12. FMOs of (TTF)(CBPQT)$(PF_6)_4$−(DNP) (**Configuration 1a**, twisted). Color code: yellow (S), red (O), blue (N), gray (C), black (H), and purple (PF_6^-).

consider the twisted conformation of (TTF)(CBPQT)$(PF_6)_4$−(DNP) as a better model for the experimental system than the planar one, and we will focus mainly on it in the analysis of the following sections. The DOSs and PDOSs of two states of the model [2]rotaxane, (TTF)(CBPQT)$(PF_6)_4$−(DNP) and (TTF)−(DNP)(CBPQT) $(PF_6)_4$, both in the twisted conformation, are shown side-by-side in Figure 11.

3.4.2. (TTF)(CBPQT)$(PF_6)_4$−(DNP) or "CBPQT@TTF". The FMOs of (TTF)(CBPQT)$(PF_6)_4$−(DNP) in the twisted conformation are shown in Figure 12 (and Figure S10 of the Supporting Information). The HOMOs are located at −5.25, −5.46, −6.69, −6.82, and −6.91 eV. The HOMO is contributed by TTF (major) and CBPQT (minor). HOMO−1, HOMO−2, and HOMO−3 are from DNP, and HOMO−4 is from TTF. The LUMO (−4.20 eV) and LUMO+1 (−3.85 eV) correspond to CBPQT slightly mixed with TTF.

While the HOMO of free TTF lies at higher energy than that of free DNP (Figures 2 and 8), the complexation of TTF with (CBPQT)$(PF_6)_4$ results in a significant **downshift** of the HOMO level of **TTF** (Figure 4), which is now **aligned** at a similar level to that of free DNP with or without the CBPQT ring nearby (Figure S9 of Supporting Information). Thus, the combination of these two stations, (TTF)(CBPQT)$(PF_6)_4$ and free DNP, leads to almost degenerate HOMO and HOMO−1 of (TTF)(CBPQT)-$(PF_6)_4$−(DNP) at −5.25 eV (from TTF) and −5.46 eV (from DNP) (Figures 11a and 12).

3.4.3. (TTF)−(DNP)(CBPQT)$(PF_6)_4$ or "CBPQT@DNP". The FMOs of (TTF)−(DNP)(CBPQT)$(PF_6)_4$ in the twisted conformation are shown in Figure 13 (and Figure S11 of the Supporting Information). The HOMOs are located at −4.54, −5.32, −6.27, −6.42, and −6.58 eV. The HOMO is mainly from TTF, while HOMO−1 and HOMO−2 are from DNP, HOMO−3 is from TTF, and HOMO−4 is from DNP. The LUMO and LUMO−1, almost degenerate (−3.90 and −3.85 eV), are from CBPQT. The contribution of DNP to these LUMO levels is negligible.

The "alignment" of HOMO energy levels corresponding to TTF and DNP described above for the "CBPQT@TTF" state is *not* the same for the "CBPQT@DNP" state. The free DNP has a lower HOMO level than free TTF (Figure 2), and the HOMO level of DNP with the ring around it is even lower (Figure 4). Thus, the combination of the free TTF and the (DNP)(CBPQT)$(PF_6)_4$ complex leads to a rather wide gap between HOMO and HOMO−1. That is, there is a "mismatch" between the HOMO (−4.54 eV from TTF) and HOMO−1

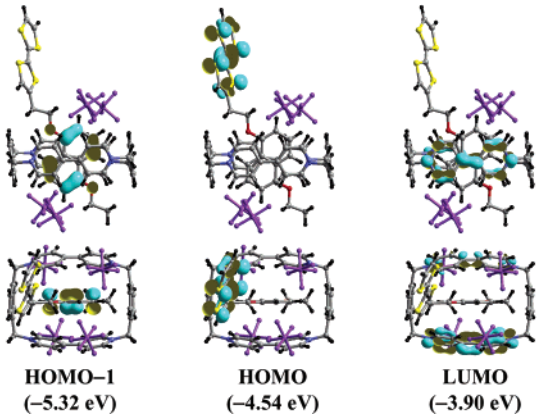

Figure 13. FMO's of (TTF)−(DNP)(CBPQT)$(PF_6)_4$ (**Configuration 1A**, twisted). Color code: yellow (S), red (O), blue (N), gray (C), black (H), and purple (PF_6^-).

(−5.32 eV from DNP) of (TTF)−(DNP)(CBPQT)$(PF_6)_4$ (Figures 11b and 13).

We note that the HOMO and the LUMO are localized at *different* stations with the HOMO exclusively at TTF and the LUMO exclusively at the CBPQT ring positioned at the DNP station and that the HOMO−LUMO gap (0.6 eV) is lower than that of the "CBPQT@TTF" state (1.1 eV) and much more lower than that of the finger only (3.6 eV).

3.5. Implication for Molecular Electronics. To analyze the mechanism of electron-tunneling through the Stoddart type [2]-rotaxanes when placed between two electrodes, we assume that the tunneling probability is likely larger when there is resonance between the two stations. Thus we expect that "the switch is on" when the energy levels of the free station and the complexed station are "aligned" to overlap (in energy) with each other within the energy window over which the current is measured, that is, in the range of $[E_F - \eta V_0, E_F + (1 - \eta)V_0]$ where E_F is the Fermi level of the electrode (say gold at −5.3 eV), V_0 is the applied voltage (usually 0.3 eV[5,8]), and η is the ratio of voltage drop across the contact between molecule and the electrode. In addition these energy levels should overlap the energy levels of the anchor to the electrodes in the energy window.

Based on this assumption, our results suggest that the role of the $(CBPQT^{4+})(PF_6^-)_4$ shuttle in switching is to "modulate" downward the energy levels of the station on which it is placed (TTF or DNP). This is due to the net positive electrostatic potential exerted by the $CBPQT^{4+}$ ring on the orbitals of the finger. This downshift alters the relative position of energy levels between TTF and DNP and in turn the electron tunneling probability between them through resonance processes, even though the $CBPQT^{4+}$ orbitals are not involved directly in the actual tunneling process. Since the magnitude of the shift is related to the net electrostatic potential on the station, it would be affected by the position of the anions (the four PF_6^-'s in our case), where separating these anions farther from the station (bigger anions or more polar solvent) would probably lead to bigger shifts. Indeed fluctuations in the anion positions (caused by mechanical, electrical, magnetic, or rheological perturbations of these anions) might lead to amplification by the device, converting it into an amplifier of the perturbing force.

The "CBPQT@TTF" state, (TTF)(CBPQT)$(PF_6)_4$−(DNP), has such "aligned" levels, thus the HOMO (TTF character;

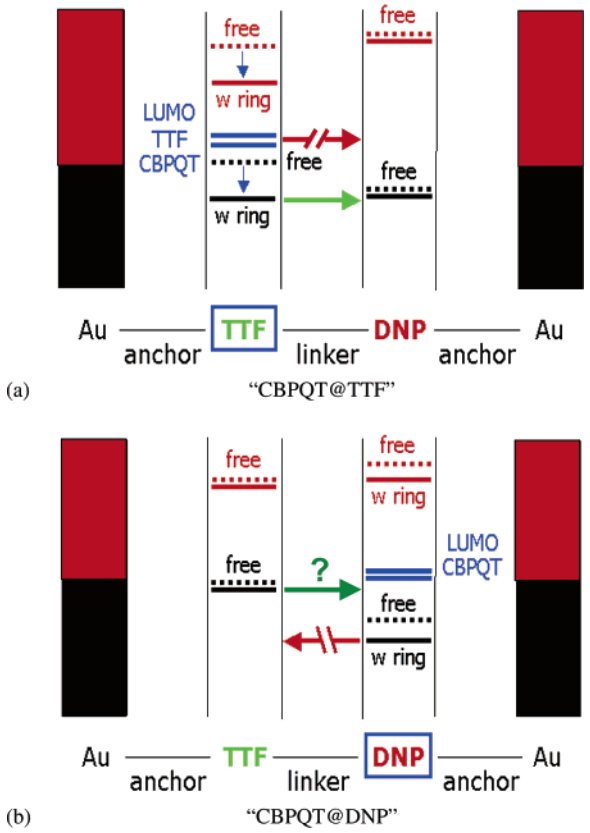

Figure 14. Schematic diagram of frontier orbital energy levels of (a) (TTF)-(CBPQT)$(PF_6)_4$−(DNP) ("CBPQT@TTF" state) and (b) (TTF)−(DNP)-(CBPQT)$(PF_6)_4$ ("CBPQT@DNP" state).

−5.25 eV) and HOMO−1 (DNP character; −5.46 eV) are nearly degenerate and correspond closely to the work function of metals (gold at −5.3 eV). [Other near degeneracies occur for the deeper level of HOMO−2 (DNP character; −6.69 eV), HOMO−3 (DNP character; −6.82 eV), and HOMO−4 (TTF character; −6.91 eV) (Figure 11a)].

On the other hand, the "CBPQT@DNP" state, (TTF)−(DNP)-(CBPQT)$(PF_6)_4$, has no such overlap near the Fermi energy. [It has only the alignment at the deep level of HOMO−2 (DNP character; −6.27 eV), HOMO−3 (TTF character; −6.42 eV), and HOMO−4 (DNP character; −6.58 eV) (Figure 11b)].

This switching mechanism suggests that the "CBPQT@TTF" state would have a much larger tunneling current than the "CBPQT@DNP" state, since it has "aligned" or overlapping energy levels which are close to E_F of the electrode and located within the energy window of V_0. Of course the means by which the rotaxane is attached to the electrode could also affect the current. The ideal anchor might have an effective Fermi energy comparable to the electrode (like an "Ohmic contact") so that it does not lead to additional tunneling impedance.

In addition there is an issue having to do with the tunneling matrix elements. If the finger was linear in the z direction perpendicular to the electrodes, we could analyze the matrix elements and tunneling in terms of σ, π_x, and π_y components (also as δ_{xy} and $\delta_{x^2-y^2}$) where π_x indicates antisymmetric through the xz plane passing through the finger. Thus it is the overlap of electrode σ orbitals to TTF's σ orbitals to DNP's σ orbitals to the second electrode's σ orbitals that leads to the σ contribution to the current and similar overlaps of π_x and π_y components that lead to the π_x and π_y contributions to the current. Since the resonating orbitals at the Fermi energy discussed above are π-like, we expect the best tunneling matrix elements to be when the planes of the TTF and DNP are parallel. In this case it is the π character of the attachment ligand (e.g., a thiol S) that is important. To whatever extent the conformation is twisted (favored by the packing energetics for our system), this matrix element should decrease, perhaps going through zero for perpendicular TTF and DNP. On the other hand a system in which a π orbital on the DNP resonates with an σ orbital on the TTF might have the largest current for a 90° orientation.

Another possible role of the $(CBPQT^{4+})(PF_6^-)_4$ shuttle in switching would be to provide low-lying LUMO levels. Here the results from the DFT calculations are less reliable, leading to quite different results for the two functionals considered here. The reduced HOMO−LUMO gap from 3.6 eV for the finger to 1.1 eV for "CBPQT@TTF" and to 0.6 eV for "CBPQT@DNP" (based on B3LYP) could conceivably facilitate the electron tunneling through the system. Again there would be issues as discussed above concerning the symmetry of the orbitals. Such direct involvement of the shuttle in the tunneling seems implausible for the ideal extended conformation (not likely to be optimum unless it is induced by packing in say a self-assembled monolayer), but it is more likely for the more realistic folded conformation in which there is direct contact between free station and the shuttle on the other station.[45,46]

For this situation with a highly folded chain, the main switching mechanism could be ON for the **"CBPQT@DNP"** state, because its HOMO−LUMO gap is smaller (that is, the HOMO and LUMO are aligned better to each other) and because the well-aligned HOMO and LUMO are localized at different stations (HOMO exclusively at TTF and LUMO at CBPQT@DNP) so that the HOMO-to-LUMO tunneling would be through the entire molecule of [2]rotaxane.

However, we do not in this paper include the electrodes or the anchors to them or the finite voltage across them, and thus any discussion on the position of E_F or the energy levels of the anchor is beyond our scope. Under application of a finite voltage across the rotaxane, the energy levels of the rotaxane might change a bit from those calculated herein. Next we will use the results from this paper to calculate the tunneling through these model [2]rotaxane compounds attached to two gold electrodes at both ends through thiolates. These calculations will use the structure and insight obtained from the current study and should determine how the "alignment" of energy levels of two stations affects the tunneling through the [2]rotaxane molecule.

3.6. PBE/6-31G.** The main text of this paper focused on DFT calculations using the B3LYP functional. In addition we carried out similar calculations at the PBE/6-31G** level in order to determine how much to trust the QM results. As shown in Figure 2, the main difference between the results is that PBE gives a significantly smaller HOMO−LUMO gap than B3LYP, a hybrid functional. The main difference involves the unoccupied orbitals which are estimated to be much too high (unbound) in the Hartree−Fock approximation but probably too stable for DFT.[47] This underestimation of the LUMO by PBE is so severe that in some cases the HOMO lies higher than the LUMO (Figure S17)! Since DFT is much less reliable for the unoc-

(46) Jeppensen, J. O.; Vignon, S. A.; Stoddart, J. F. *Chem.—Eur. J.* **2003**, *9*, 4611−4625.
(47) Nitzan, A. *Annu. Rev. Phys. Chem.* **2001**, *52*, 681−750.

cupied levels than for the occupied ones,[47] we do not emphasize their quantitative nature (exact energy levels, for example). Thus, even in the "reversed-order" cases, we assume that the energy levels remain correct up to the HOMO. Thus from PBE DFT, we draw the same conclusions on the nature of the rotaxanes, "conservation of identity" (Figure S12), "downshift of station levels by CBPQT", "stronger interaction of CBPQT with TTF than with DNP" (Figure S13), "downshift of free station by CBPQT when they are closely located" (Figure S14), but as shown in Figures S16 and S17, the alignment scheme, which is rather quantitative, is not exactly the same in the two cases.

Summary

We used density functional theory (B3LYP/6-31G** and PBE/6-31G**) to study the electronic structure of the Stoddart−Heath type [2]rotaxane, one of the most promising molecular switches being developed. Although there are some quantitative differences in the LUMO energy levels, they show such common features as follows:

(1) The electronic structure of [2]rotaxane can be constructed reasonably well by combining the energy levels of the separate stations (TTF and DNP) with or without the $(CBPQT)(PF_6)_4$ shuttle around them. That is, the "CBPQT@TTF" state, $(TTF)(CBPQT)(PF_6)_4-(DNP)$, is described well with a combination of the $(TTF)(CBPQT)(PF_6)_4$ complex and free DNP, and the "CBPQT@DNP" state, $(TTF)-(DNP)(CBPQT)(PF_6)_4$, with a combination of free TTF and the $(DNP)(CBPQT)(PF_6)_4$ complex. This aufbau or "bottom-up" approach allows us to understand the more complicated [*n*]rotaxanes based on knowledge about each piece and should be useful in designing new stations and rings.

(2) We find that the $(CBPQT^{4+})(PF_6^-)_4$ shuttle induces a downshift (more stable) in the frontier orbital energy levels of the station on which it is located (TTF or DNP), due to the net positive electrostatic potential exerted by the $CBPQT^{4+}$ ring. This downshift alters the relative position of energy levels between TTF and DNP and in turn the electron tunneling probability between them, even though the ring itself is not involved directly in the actual tunneling process. Thus the $CBPQT^{4+}$ serves as a switch that turns on the TTF state by moving its orbitals to the Fermi energy of the electrode to overlap those of the DNP and turns off the DNP state by moving its orbitals away from each other. This mechanism predicts that the "CBPQT@TTF" state is a better conductor, since it has better aligned levels between two stations. This mechanism is most likely to apply to cases in which the chain is extended as in the drawing **1**.

(3) A second possible role of the $(CBPQT^{4+})(PF_6^-)_4$ shuttle in switching is to provide low-lying LUMO levels. If there are good matrix elements involving the CBPQT's LUMO orbitals, the reduced HOMO−LUMO gap [from 3.6 eV for the thread only to 1.1 eV ("CBPQT@TTF") or to 0.6 eV ("CBPQT@DNP") in B3LYP] would significantly facilitate the electron tunneling through the system. This could be the situation for a folded conformation, where direct contact between the free station and the shuttle on the other station is possible. When this is the main switching mechanism, the "CBPQT@DNP" state is expected to be a better conductor, both because its HOMO−LUMO gap is smaller but also because its HOMO and LUMO are localized at different stations (HOMO exclusively at TTF and LUMO at CBPQT@DNP) so that the HOMO-to-LUMO tunneling would be through the entire molecule of [2]rotaxane.

This validation and elaboration of the Aufbau approach to understanding the properties of the composite rotaxane in terms of the components (stations and ring modulator) should be useful in guiding the design of new stations, modulators, and the attachment strategies to electrodes. In addition the structures and interpretation obtained from this work should be useful in calculating how the tunneling current between two electrodes depends on configuration and attachment to the electrode.

Acknowledgment. We thank Prof. J. Fraser Stoddart and his research group at UCLA for stimulation and helpful discussion. We also thank Prof. James Heath of Caltech for helpful discussions. This work was partially supported by the National Science Foundation [NIRT] and by MARCO-FENA. In addition, the facilities of the MSC were supported by ONR-DURIP, ARO-DURIP, NSF-MRI, and IBM (SUR Grant).

Supporting Information Available: The detailed results obtained with PBE/6-31G** and the electronic structures of the alternative configurations. This material is available free of charge via the Internet at http://pubs.acs.org.

JA0385437